Enhancing ionic conductivity of bulk single-crystal yttria-stabilized zirconia by tailoring dopant distribution

Eunseok Lee, Friedrich B. Prinz, and Wei Cai

Department of Mechanical Engineering, Stanford University, Stanford, California 94305, USA

We present an *ab initio*–based kinetic Monte Carlo model for ionic conductivity in single-crystal yttria-stabilized zirconia. Ionic interactions are taken into account by combining density functional theory calculations and the cluster expansion method and are found to be essential in reproducing the effective activation energy observed in experiments. The model predicts that the effective energy barrier can be reduced by 0.15–0.25 eV by arranging the dopant ions into a superlattice.

Yttria-stablized zirconia (YSZ) is a widely used electrolyte in solid oxide fuel cells (SOFC) and oxygen sensors because of its high ionic conductivity at high temperatures.[1] Driven by the need to reduce the operating temperature of SOFC, much of the current research effort focuses on the design of new solid electrolyte materials with significantly enhanced ionic conductivity at intermediate temperatures.[2,3] The presence of free surfaces in nanoscale thin films and interfaces in hetero-epitaxial structures has been found to enhance ionic conductivity.[4–9] However, the effect of dopant distribution on the ionic conductivity of bulk single-phase electrolytes has largely remained unexplored, despite the fundamental importance of dopant-vacancy interaction in ionic transport[10,11] and the possibility of tailoring dopant distributions by novel deposition techniques.[12]

Atomistic simulations have the promise to become a useful design tool for new electrolyte materials, by predicting the ionic conductivity of candidate structures and elucidating the fundamental transport mechanisms.[11,13–17] Unfortunately, they are still limited in their length and time scales. For example, to accurately describe the long-range ionic interactions in YSZ requires density functional theory (DFT) models with relatively large supercells. The high computational cost limits the time scale of *ab initio* molecular dynamics simulations to picoseconds.[14] Hence, a major challenge at present is to construct a kinetic Monte Carlo (kMC) model that not only can access the macroscopic time scale[16,17] but also retains the accuracy of DFT models in describing the ionic interactions. In the pioneering kMC model for YSZ,[16] ionic interactions are ignored in the metastable states; i.e., all possible states are sampled with uniform probability. While it successfully predicts a maximum in the conductivity as a function of doping concentration, the predicted temperature dependence is significantly weaker than found in experiments, signaling the importance of ionic interactions. The lack of ionic interaction also makes this model unsuitable to predict the effect of dopant distribution on ionic conductivity.

In this Brief Report, we develop a kMC model for oxygen vacancy diffusion in YSZ that faithfully captures the ionic interactions. DFT calculations with supercell sizes significantly larger than previous studies[16,18] are performed to accommodate long-range interactions, and the data are used to construct a cluster expansion (CE) model. Kinetic Monte Carlo simulations using this model predict an effective

activation energy that agrees better with experiments than the noninteracting model. The kMC simulations further predict that the maximum conductivity is achieved when the yttrium dopant ions are distributed as [100] lines and form a two-dimensional (2D) rectangular superlattice in the two other directions. The effective energy barrier in this structure is lower than the random distribution by 0.15–0.25 eV.

Ionic conduction in YSZ occurs through oxygen anion diffusion by the vacancy mechanism. The ionic conductivity is the averaged effect of many vacancy jumps and can be predicted from a kMC simulation over a sufficiently long time. The degrees of freedom in our kMC model are the positions of the oxygen vacancies, which hop on the simple cubic anion sublattice of YSZ. At each kMC step, the probability rates of all vacancy jumps to their nearest neighbor positions are calculated by $j = \nu_0 \exp(-\frac{E_b}{k_B T})$, where k_B is Boltzmann's constant, T is temperature, and E_b is the activation energy barrier for each jump. The jump trial frequency ν_0 is set to 10^{13} Hz.[16] At each step, only one event is selected based on the probability rates of all possible events.[19] From a long kMC simulation, the diffusion coefficient of the vacancies center of mass is computed from the mean-square displacement. The ionic conductivity is then computed from the Nernst-Einstein relation.[20]

A fundamental input to the kMC simulation is the energy barriers for vacancy jumps, E_b, which depend on the ionic configurations around the jumping vacancy. Because on-the-fly determination of energy barriers[21] from first principles is prohibitively expensive, a computationally efficient energy barrier model is needed. In a previous model,[16] E_b is assumed to depend only on the chemical species of the two cations closest to the jumping vacancy, as shown in Fig. 1(a). Because the energy barrier of every jump equals that of the reverse jump, one can show that all metastable states in this model must have identical energy. Hence we will refer to it as the *noninteracting* model. Experimental and computational data have suggested that interactions play an important role in ionic conduction.[10,11] To account for interactions, we use the kinetically resolved activation (KRA) model,[22,23] in which $E_b = f(E_b^0, \Delta E)$, where E_b^0 is the "kinetically resolved" barrier when the two metastable states happen to have identical energy, and ΔE is the energy difference between the two states. We take the energy barriers in the noninteracting model[16] as our E_b^0. The function f is often approximated by $E_b = E_b^0 - \Delta E/2$.[22,23]
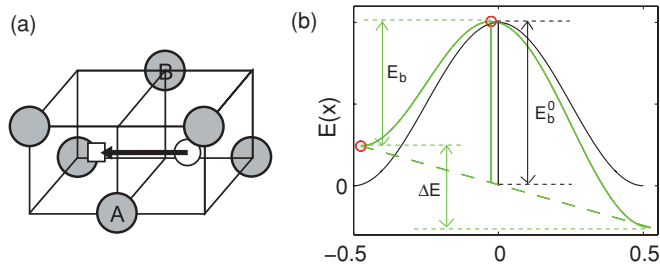
FIG. 1. (Color online) (a) In the noninteracting model E_b depends only on whether cations A and B are Zr or Y. $E_b = 0.58$, 1.29, or 1.86 eV if within pair A-B there are 0, 1, or 2 Y cations.[16] Filled circles represent cations, the open circle represents the oxygen anion, and the open square represents the oxygen vacancy. (b) In our interacting model, the energy difference ΔE between the initial and final state is assumed to modify the energy profile of the vacancy jump by superimposing a linear function.

Here we use a slightly better approximation for function f by assuming that the energy landscape between the two metastable states has a sinusoidal shape when $\Delta E = 0$ and is modified by a linear term when $\Delta E \neq 0$.[20] Hence our task of specifying the energy barrier E_b is reduced to an accurate description of the energy difference ΔE.

Because the ionic interactions in YSZ are long ranged, they can only be captured accurately by DFT calculations in relatively large supercells. It is impossible to perform DFT calculations for all ionic configurations sampled by the kMC simulation. Instead, we use the cluster expansion method (CEM) to limit the necessary number of DFT calculations. In the CEM, every metastable state in the kMC simulation can be uniquely mapped to a spin configuration $\{s_i\}$ of an Ising model.[18] The energy as a function of ionic configuration can be expressed by a cluster expansion[24]

$$E(\{s_i\}) = \sum_\alpha V_\alpha \phi_\alpha(\{s_i\}), \qquad (1)$$

where V_α is called effective cluster interaction (ECI) for cluster α, and $\phi_\alpha = \prod_{i \in \alpha} s_i$ is the cluster function involving all spin variables belonging to cluster α. Equation (1) is used to compute the energy of any metastable state encountered by the kMC simulation, prior to which the ECI coefficients V_α's are fitted to a DFT data set.

To construct the *ab initio* database for the fitting, we performed DFT calculations for 140 randomly chosen ionic configurations within a $3[100] \times 3[010] \times 3[001]$ YSZ super-cell, using the Vienna Ab-initio Simulation Package (VASP).[25] This supercell contains 108 cation sites (Zr or Y) and 216 anion sites (O or oxygen vacancy) and is significantly larger than previous studies,[16,18] in order to accurately account for long-range Coulombic and elastic interactions. K-point sampling is limited to the Γ point by considering the large size of the supercell. The volume and the shape of the supercell are allowed to relax together with the ionic positions. A high energy cutoff of 520 eV is used to avoid Pulay stress. Each ionic configuration takes $\sim 10^4$ CPU-hours to be fully relaxed.

The number of clusters needs to be significantly truncated for robust fitting; otherwise the cluster expansion model can be overly adapted to the fitted data set.[26] First, we only keep the clusters in which any two spins are separated by

less than $1.5a_0$, where a_0 is the lattice parameter of YSZ. Second, we only keep clusters that involve up to three spins. By accounting for the translational and rotational symmetries, 192 independent clusters survive this truncation. For further truncation, a Monte Carlo algorithm is used to select n_c clusters out of 192 possible clusters by minimizing the cross-validation score.[18] To measure the predictive power of the CEM, we separate the DFT data into two sets. Set I contains 100 data points and these are used to fit the ECIs. Set II contains 40 data points and these are used to benchmark the CEM's predictions. The root-mean-square difference between the DFT energies and the CEM's predictions per cation in Set I and Set II are defined as the error of fitting and the error of prediction, respectively.

These two errors have different dependence on n_c. For example, when $n_c = 97$, the error of fitting is 0.0006 eV while the error of prediction is 0.012 eV. The large difference between the two errors means that the fitted CEM has entirely lost its predictive power if n_c is too large. Only when $n_c \leqslant 9$, both errors are the same and they decrease with increasing n_c. Hence, in this work, the optimal choice is $n_c = 9$, where both the error of fitting and the error of prediction is 0.005 eV, as shown in Fig. 2.[20] This error is small enough for our kMC simulations and is smaller than a previous study.[18] To our knowledge this is the first time the predictive power of an interaction model for YSZ has been demonstrated by monitoring the error of prediction. Figure 2(b) shows the effective binding energy between an Y ion and an oxygen vacancy predicted by the CEM model. The preference of the oxygen vacancy to the second nearest neighbor site of Y is clearly seen, consistent with previous experimental and theoretical works.[16,17]

The fitted CEM allows us to compute the energy difference ΔE between the two states before and after a vacancy jump,
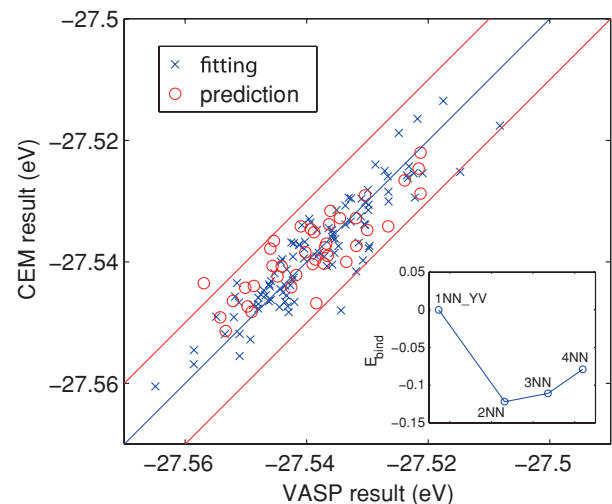

FIG. 2. (Color online) The 140 data points are divided into two sets: Set I contains 100 data points ($\times$) and is used to fit the CEM, set II contains 40 data points ($\circ$) and is not included in the fit. Energies predicted from the CEM are plotted against energies computed from DFT using VASP, in units of eV per cation. The inset shows the effective binding energy between Y and the oxygen vacancy predicted by the CEM.
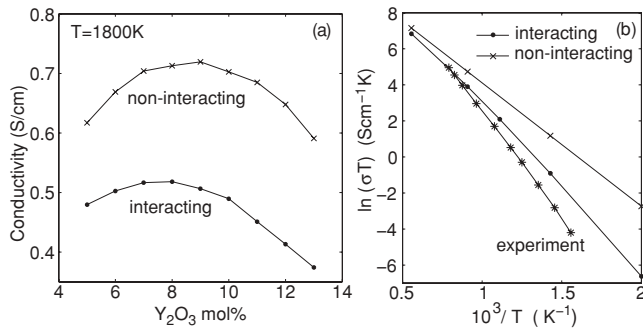
FIG. 3. (a) Conductivity of a YSZ single crystal predicted by kMC simulations at $T = 1800$ K as a function of doping concentration. (b) Predicted temperature dependence of YSZ conductivity at 8-mol% doping concentration. Y dopant cations are assumed to be randomly distributed. Experimental data are reproduced from Ref. 28.

which modifies the energy barrier E_b of the jump. Using this energy barrier model, we performed kMC simulations in $3[100] \times 3[010] \times 3[001]$ YSZ supercells in which the doping concentration varies from 5% to 13%. The ionic conductivity at each doping concentration is computed by averaging over 40 randomly generated Y distributions. As shown in Fig. 3(a), the ionic conductivity (at 1800 K) is maximum at 8 mol%, consistent with earlier experimental[27,28] and theoretical results.[16,17] Figure 3(b) is the Arrhenius plot of ionic conductivity at 8-mol% doping concentration. The predicted activation energy is 0.74 eV at high T and 0.85 eV at low T, in much better agreement with experiments (0.85–1.0 eV)[28] than the noninteracting model (0.59 eV).[16] The remaining difference with experiments may be due to the error in E_b^0 taken from Ref. 16. The neglect of activation entropy in vacancy jumps does not affect the conclusion because it does not change the slope of the Arrhenius plot.

The conductivity results shown in Fig. 3 are the averaged value over 40 random Y configurations, the standard deviation over which is about 19% of the average. This indicates that the ionic conductivity is sensitive to the spatial distribution of Y cations and poses the following question: What is the optimal Y distribution that maximizes ionic conductivity? To answer this question, we have performed kMC simulations for a variety of Y distributions, in which the Y cations are segregated into spherical clusters, (001) layers, or [100] rods. The simulation results suggest two design principles that ultimately guide us to the optimal Y distribution.

When all Y cations in the supercell are segregated into a spherical cluster, the ionic conductivity is actually lower than the random distribution (by 27% at 1800 K), contrary to the prediction based on the noninteracting model.[15] This is because the interaction between Y cations and oxygen vacancies, as shown in Fig. 2, attracts the vacancies next to the cluster. To diffuse over long distances and contribute to the ionic conductivity, vacancies must detach from the Y clusters. This requires overcoming a binding energy of $\sim$0.12 eV, which reduces the ionic conductivity.

Here the reduction of ionic conductivity is caused by the increase of spatial variation of the potential energy. Based on this result, we can formulate *design principle* I: The optimal

Y distribution should minimize the energy variation of the metastable states as oxygen vacancies jump along the conduction direction. In this work, we focus on conduction along the [100] (i.e., x) direction. A promising candidate structure is to have Y cations segregated into planes, so that each (001) cation layer is either completely filled by Y or completely filled by Zr. Due to translational invariance, the potential energy from cation-vacancy interaction remains constant after an oxygen vacancy jumps in the [100] direction.[29] The layered structure can be fabricated using thin-film-deposition techniques such as pulsed laser deposition.[12]

Unfortunately, the layered structure also has a lower conductivity than the random distribution (by 59% at 1800 K). This is surprising because one might expect enhanced conductivity, as the noninteracting model would predict, due to the existence of Y-free channels. The reduction in conductivity is caused by the segregation of oxygen vacancies to the two anionic layers immediately next to the Y layer. Because there is always a first nearest neighbor (1nn) Y, vacancy diffusion in this layer experiences a high energy barrier (with $E_b^0 = 1.29$ eV). Given that vacancies prefer to be the second nearest neighbors (2nn) of Y, as shown in Fig. 2, it is somewhat surprising that the vacancies segregate to the nearest anionic layer. This problem is resolved by noticing that when the vacancy becomes the 1nn of two Y cations, it becomes the 2nn to four Y cations on the same cation layer. This result motivates our *design principle* II: The optimal Y distribution should not induce a high oxygen vacancy density in the first nearest neighbor sites of any Y cations.

It turns out that the design principles I and II can be simultaneously satisfied when Y cations are segregated into [100] lines. When Y lines are well separated from each other, kMC simulations show that the oxygen vacancy density is peaked at 2nn sites surrounding the Y lines. To enhance conductivity, we would like to pack more Y lines per unit volume in order to enhance the overall vacancy density. But when the distance between Y lines becomes too small, oxygen vacancies start to occupy 1nn sites around Y, deteriorating the ionic conductivity.

We examined a variety of 2D structures formed by [100] Y-segregated lines. The optimal structure at 1800 K is a square lattice with periodicity $1.5a_0$ in y and z directions (structure A). Interestingly, the optimal structure at 500 K is different; it is a rectangular lattice with periodicity $1.5a_0$ and $2a_0$ in y and z directions, respectively (structure B). In both structures, the vacancy concentration is high in fast-diffusing channels ($E_b^0 = 0.58$ eV) away from 1nn sites of Y [see Fig. 4(a)].

Figure 4(b) shows a plot of the temperature dependence of conductivity for structures A and B. Their activation energy is around $\sim$0.6 eV, significantly lower than the random distribution. Compared with the random Y distribution (at 8 mol%), the ionic conductivity of structure A is enhanced by a factor of 1.35 at 1800 K, 11 at 500 K, and 86 at 300 K. For structure B, the enhancement factor is 22 at 500 K and 532 at 300 K. This result provides a theoretical upper limit of ionic conductivity that can be achieved by rearranging dopants in YSZ.

In summary, we have developed an *ab initio*–based kMC model of the vacancy diffusion in bulk YSZ that accurately
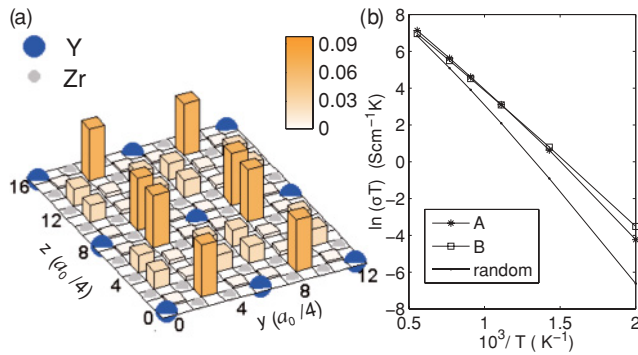
FIG. 4. (Color online) (a) Vacancy distribution in structure B at $T = 500$ K. Blue and gray circles indicate Y and Zr, respectively. The darker color in the orange columns corresponds to higher vacancy concentration. (b) Temperature dependence of the conductivity at different Y distributions. A random Y distribution corresponds to a doping concentration of 8 mol%.

accounts for the ionic interactions. The predicted ionic conductivity shows much better agreement with experiments regarding the temperature dependence than the noninteracting model. The model predicts strong dependence of ionic conductivity on the spatial distribution of dopant cations. The maximum conductivity is reached when Y cations are arranged into a rectangular superlattice of [100] lines. Fabrication of this structure is challenging, but may be feasible with novel deposition techniques. The method presented here can be easily applied to other solid electrolytes, in which the optimal dopant microstructure may be different from that in YSZ and may be easier to synthesize.

[1] R. O'Hayre, S.-W. Cha, W. Colella, and F. B. Prinz, *Fuel Cell Fundamentals* (Wiley, New York, 2006), Chap. 7.
[2] S. Hui *et al.*, J. Power Sources **172**, 493 (2007).
[3] B. Steele and A. Heinzel, Nature (London) **414**, 345 (2001).
[4] G. Knöner *et al.*, Proc. Nat. Acad. Sci. USA **100**, 3870 (2003).
[5] R. Souza *et al.*, Phys. Chem. Chem. Phys. **10**, 2067 (2008).
[6] N. Sata *et al.*, Nature (London) **408**, 946 (2000).
[7] I. Kosaki *et al.*, Solid State Ionics **176**, 1319 (2005).
[8] J. Garcia-Barriocanal *et al.*, Science **321**, 676 (2008).
[9] N. Schichtel *et al.*, Phys. Chem. Chem. Phys. **11**, 3043 (2009).
[10] G. Stapper, M. Bernasconi, N. Nicoloso, and M. Parrinello, Phys. Rev. B **59**, 797 (1999).
[11] F. Pietrucci, M. Bernasconi, A. Laio, and M. Parrinello, Phys. Rev. B **78**, 094301 (2008).
[12] C. Chao, Y. Kim, and F. Prinz, Nano Lett. **9**, 3626 (2009).
[13] T. Sayle, S. Parker, and D. Sayle, J. Mater. Chem. **16**, 1067 (2006).
[14] T. J. Pennycook, M. J. Beck, K. Varga, M. Varela, S. J. Pennycook, and S. T. Pantelides, Phys. Rev. Lett. **104**, 115901 (2010).
[15] E. Lee, F. Prinz, and W. Cai, Electrochem. Comm. **12**, 223 (2010).
[16] R. Krishnamurthy *et al.*, J. Am. Ceram. Soc. **87**, 1821 (2004).
[17] R. Pornprasertsuk *et al.*, J. Appl. Phys. **98**, 103513 (2005).
[18] A. Predith, G. Ceder, C. Wolverton, K. Persson, and T. Mueller, Phys. Rev. B **77**, 144104 (2008).
[19] A. B. Bortz, M. H. Kalos, and J. L. Lebowitz, J. Comput. Phys. **17**, 10 (1975).
[20] See supplemental material at [http://link.aps.org/supplemental/10.1103/PhysRevB.83.052301].
[21] J. L. Bocquet, Defect and Diffusion Forum: Annual Retrospective IV **203–205**, 81 (2002).
[22] A. Van der Ven, G. Ceder, M. Asta, and P. D. Tepesch, Phys. Rev. B **64**, 184307 (2001).
[23] A. Van der Ven and G. Ceder, Phys. Rev. Lett. **94**, 045901 (2005).
[24] P. D. Tepesch, G. D. Garbulsky, and G. Ceder, Phys. Rev. Lett. **74**, 2272 (1995).
[25] G. Kresse and J. Furthmüller, Phys. Rev. B **54**, 11169 (1996).
[26] J. Rosen *et al.*, Comput. Optim. Appl. **17**, 329 (2000).
[27] A. I. Ioffe, D. Rutman, and S. Karpachov, Electrochim. Acta **23**, 141 (1978).
[28] S. Ikeda *et al.*, J. Mater. Sci. **20**, 4593 (1985).
[29] The vacancy-vacancy interaction can still induce a small energy variation.